Analyte chemisorption and sensing on *n*- and *p*-channel copper phthalocyanine thin-film transistors

Richard D. Yang,[1,a)] Jeongwon Park,[1] Corneliu N. Colesniuc,[2] Ivan K. Schuller,[2] James E. Royer,[3] William C. Trogler,[3] and Andrew C. Kummel[3,b)]

[1]*Materials Science & Engineering, University of California, San Diego, La Jolla, California 92093, USA*
[2]*Department of Physics, University of California, San Diego, La Jolla, California 92093, USA*
[3]*Department of Chemistry and Biochemistry, University of California, San Diego, La Jolla, California 92093, USA*

Chemical sensing properties of phthalocyanine thin-film transistors have been investigated using nearly identical *n*- and *p*-channel devices. *P*-type copper phthalocyanine (CuPc) has been modified with fluorine groups to convert the charge carriers from holes to electrons. The sensor responses to the tight binding analyte dimethyl methylphosphonate (DMMP) and weak binding analyte methanol (MeOH) were compared in air and N_2. The results suggest that the sensor response involves counterdoping of pre-adsorbed oxygen (O_2). A linear dependence of chemical response to DMMP concentration was observed in both *n*- and *p*- type devices. For DMMP, there is a factor of 2.5 difference in the chemical sensitivity between *n*- and *p*-channel CuPc thin-film transistors, even though it has similar binding strength to *n*- and *p*-type CuPc molecules as indicated by the desorption times. The effect is attributed to the difference in the analyte perturbation of electron and hole trap energies in *n*- and *p*-type materials. © 2009 American Institute of Physics.
[DOI: 10.1063/1.3078036]

I. INTRODUCTION

Organic thin-film transistors (OTFTs) are a form of chemically sensitive field-effect transistors (ChemFETs).[1] ChemFETs have advantages in multiparameter readouts[2] and offer potentially higher chemical sensitivity in comparison to chemiresistors.[3] ChemFETs can have higher electrical conductivity as compared to two-terminal chemiresistors; very thin monolayer (ML) FET devices may be fabricated to enhance the chemical sensitivity and baseline stability.[4] Metal phthalocyanine (MPc) based ChemFETs have been investigated for detecting O_3,[5] volatile organic vapors (VOC), and explosive agent simulants.[4] MPc ChemFETs may also offer improved selectivity for chemical sensing. Chemical interactions between analytes and MPc molecules are tunable by either changing the metal centers or the peripheral ligands of the macrocycle molecular structure. Combinatorial MPc ChemFET arrays (M=Cu, Zn, Ni, and Co) were reported recently for VOC detection.[6] Despite intensive study of OTFTs in chemical sensing, the transduction mechanism of ChemFETs is not fully understood.[7,8] In this report, the chemical sensing mechanism is investigated by comparing the responses of analogous *n*- and *p*-channel MPc Chem-FETs. The charge carriers for *n*- and *p*-channel devices are electrons and holes, respectively.

Copper phthalocyanine (CuPc) is a *p*-channel material. Perfluorination of CuPc to $F_{16}CuPc$ changes the charge carriers from holes to electrons. Dimethyl methylphosphonate (DMMP), a simulant for the chemical warfare agent sarin,[9] is investigated as a model tight binding analyte to MPc molecules, and methanol is investigated as a model weak binding analyte. MPc sensors were previously investigated for detecting organophosphonate nerve gas simulants.[10–12] The tight and weak binding analytes were selected based on data for chemical sensitivity and recovery times of the analytes on MPc ChemFETs with completely recoverable baselines;[4] in contrast, most previous studies on MPc sensors employed redox active analytes such as NO_2, NH_3, and O_3, which irreversibly react with MPc films at higher concentration.[26] The classical MPc chemical sensor studies explain the sensor transduction mechanism based on electron donor and acceptor interactions between analyte and MPc molecules, which continues to be the basis for many chemical sensor designs.[13] Oxygen (O_2) doping has been identified as the critical factor in the function of the solid-state MPc ChemFETs. The roles of oxygen surface doping in the electrical conductivity and chemical response were studied by comparing measurements between *n*- and *p*-channel devices in air and nitrogen carrier gases.

II. EXPERIMENTAL

CuPc and copper-hexadecafluorophthalocyanine ($F_{16}CuPc$) were purchased from Sigma-Aldrich and purified by zone sublimation. The molecular structures of CuPc and $F_{16}CuPc$ are shown in Fig. 1. The CuPc material was purified by three zone sublimation at 400 °C over 60 h with a yield over 70%. The $F_{16}CuPc$ material required over 100 h of purification (4 cycles at 400 °C) and the yield after sublimation was below 10%. The low yield in purifying $F_{16}CuPc$ by sublimation has been noted by others.[14] However, good quality

a)Present address: Applied Materials, Santa Clara, CA 95052.
b)Electronic mail: akummel@ucsd.edu.
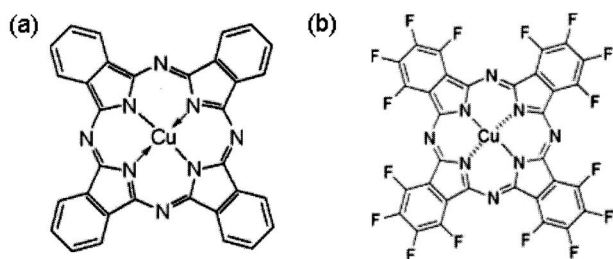
FIG. 1. The molecular structures of CuPc (a) and F_{16}CuPc (b) channel materials for ChemFETs.

FIG. 2. (Color online) Output characteristics CuPc (a) and F_{16}CuPc (b) transistors. The gate oxide is 100 nm thick SiO_2. The channel length is 5 μm. The channel widths are 50 and 400 mm for the p- and n-channel devices, respectively.

thin-films[15] and well-behaved OTFT characteristics have been reported with F_{16}CuPc channels.[16–18] Both CuPc and F_{16}CuPc films were deposited by organic molecular beam deposition at 80 °C at rates between 0.3 to 0.5 Å/s. Both films were about 30 ± 5 nm thick. The ChemFET device structure and fabrication processes have been described elsewhere.[19] Briefly, the channel length was defined by photolithography to be 5 μm. The gate dielectric was 100 nm thick thermally grown SiO_2. Interdigitated source and drain electrodes were used to increase the channel width and the drain current. The channel widths were 50 and 400 mm for the p- and n-channel devices, respectively. The carrier mobility of the CuPc device is typically about ten times higher than that of the F_{16}CuPc device, as reported previously.[16] The mobility of CuPc and F_{16}CuPc devices shown in Fig. 3 are 1.5×10^{-4} and 1.2×10^{-5} cm^2/V s, respectively, in the saturated region. The longer channel width of the F_{16}CuPc device, as compared to the CuPc device, ensured that the two devices had comparable drain currents at the same magnitudes of drain and gate biases.

Electrical properties of the OTFTs were measured using a Keithley 6385 picoammeter and programmable Agilent E3631A power supply. The electrical measurement system was calibrated with an HP 4156B precision semiconductor parameter analyzer. Output characteristics of the CuPc and F_{16}CuPc devices were measured in air before analyte exposure to ensure the proper behavior of the ChemFETs. CuPc has a highest occupied molecular orbital level (5.3 eV) close to the gold work function (5.0 eV) and is known to be a good hole transport material. The peripheral fluorine groups in F_{16}CuPc withdraw electrons from the CuPc molecule, lowering the lowest unoccupied molecular orbital level (4.8 eV) for electron injection from gold electrodes.[20] The transistor output curves (see Fig. 2) show p- and n-channel formations for the CuPc and F_{16}CuPc devices, consistent with literature reports.[16,17,21]

The chemical sensing mechanism was investigated with the tight binding analyte (DMMP) and the weak binding analyte methanol (MeOH). Other analytes, such as di-isopropyl methylphosphonate (DIMP), H_2O, and nitrobenzene, were also tested for comparison of chemical sensitivities. Analytes were delivered by a custom built flow system with a stainless steel chamber. The dead volume was 45 cm^3. The total flow rate through the chamber was 500 SCCM (SCCM denotes cubic centimeter per minute at STP). The temperature in the chamber was kept at 25 °C using a Haake constant tempera-

ture bath to circulate coolant through the chamber walls. Ultrahigh purity dry air or dry N_2 was used as both the purge and the carrier gas. Bubblers filled with liquid analytes were kept in a water bath at 25 °C. Mass flow controllers were used to dilute and introduce vaporized analytes into a manifold to premix with the carrier gas before flowing into the test chamber. Solenoid valves before and after the analyte bubblers were used to prevent cross contamination between analytes. To ensure that there was neither vapor loss nor condensation in our delivery lines, the response versus analyte concentration was measured; at low concentration, the response is linear with concentration consistent with the integrity of the vapor delivery system. The DMMP vapor pressure was cited from the work of Hopkins and Lewis.[9] A dosing calibration was performed using gas chromatography-mass spectrometer (GC/MS) (ThermoFinnigan). The exhaust from the chamber was bubbled through methanol at ~-70 °C to trap the DMMP vapor (m.p.$_{DMMP}=-50$ °C). The resulting methanol/DMMP mixture was analyzed using the integrated areas of the chromatogram peaks corresponding to 79.1m/z, 94.1m/z, and 109.2m/z. The integrated areas from these samples were compared to integrated areas for calibrated samples prepared by serial dilution. The expected dosing concentration using the published DMMP vapor pressure was found to agree with the concentration determined by GC/MS to within 40%. For all sensitivity studies, the published DMMP vapor pressures were employed since small amounts of condensation may have caused errors in the calibration experiment.

Once exposed to the atmosphere, all the sensor thin films are doped by atmospheric gases such as O_2, O_3, and H_2O. The organic ChemFETs in this study are not pristine devices, since the channel conductivity changed after exposing to the atmosphere. For these MPc ChemFETs, it was found that stable electrical conductivity and chemical response are only attainable after aging in air for at least 1 month. The devices in this study were aged under atmospheric conditions for 6 months before testing. The change in the electrical properties of MPc ChemFETs during aging is attributed to the aging of MPc/Au contacts; however, the electrode shape can also affect the electrical properties.[22] The ChemFETs were mounted on a custom-designed printed circuit board (PCB). Indium was used as solder to connect source and drain electrodes to the PCB contact pads. All devices were annealed at 55 °C in dry air for 3 h and stabilized in the optically sealed chamber overnight under a dry air flow before the chemical sensing measurements. This procedure minimized doping with atmospheric H_2O. The pulsed gating technique[19] (0.1 Hz, 1% duty cycle) was used for all chemical response measurements to mitigate bias-stress effects[23] on baseline stability. Chemical responses to DMMP and methanol doses were compared under dry air and N_2 carrier gases. The devices were measured in the saturation region at the same electrical field strength for *n*- and *p*-channel ChemFETs ($V_{ds}=6$ V, $V_{gs}=8$ V), unless otherwise stated. The bias is positive for the *n*-channel device and negative for the *p*-channel device. The chemical sensing measurements were repeated three times on *n*- and *p*-channel ChemFETs unless otherwise stated. For each type of ChemFET, we compared the chemical responses to DMMP and MeOH between duplicate devices on the same substrate and found good reproducibility ($\pm 25\%$).

The devices were intensively tested over 2 months (continuously biased at the drain electrode and exposed to analytes). For the above analytes, the *n*- and *p*-channel ChemFETs have good chemical stability and reproducible chemical responses from run to run ($\pm 10\%$). The drain current may decrease up to 50% over 2 months under intensive testing, which was typically due to the degradation of indium soldering between source and drain electrodes and the contact pads of the PCBs. To minimize the electrical contact degradation, the chemical sensing data for side-by-side device comparisons were acquired within 2 weeks, unless otherwise stated.

III. RESULTS AND DISCUSSION

A. The role of oxygen surface doping in channel conductivity

Since the channel conductivities of all the MPc ChemFETs change significantly when exposed to ambient air after deposition in vacuum, we hypothesize that the MPc films are doped with atmospheric dopants. To elucidate the effect of oxygen doping, the channel conductivities and sensing properties of the *n*- and *p*-type films were compared in dry air and dry N_2. Before all measurements, the devices were left in the dosing chamber under dry air for at least 24 h in the dark to minimize H_2O and photocurrent doping. To
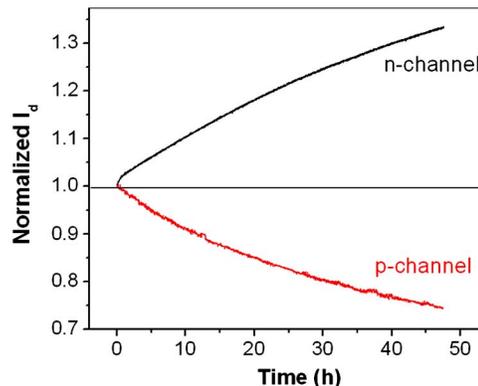
FIG. 3. (Color online) Time evolution of the *n*- and *p*-channel normalized drain currents in dry N_2 measured in saturated region. The bias conditions: *n*-channel ($V_{ds}=+6$ V, $V_{gs}=+10$ V), *p*-channel ($V_{ds}=-6$ V, $V_{gs}=-10$ V). The chamber temperature was kept at 25 °C.

understand the role of oxygen doping, the time evolution of the *n*- and *p*-channel devices were monitored after removing the oxygen from the environment and flowing dry N_2 over the devices. Figure 3 displays the drain currents for CuPc and $F_{16}CuPc$ ChemFETs over 50 h in dry N_2. Occasionally, a fast initial current change was observed; the current shown in Fig. 3 was recorded 20 min after switching to N_2. The 20 min delay removes any transient responses due to temperature or pressure changes from carrier gas switching. The drain current increased 34% for the *n*-channel device and decreased 26% for the *p*-channel device after 50 h under a nitrogen atmosphere. The 50 h experiment was performed only once, but similar experiments of 4–5 h duration have been conducted more than ten times and those results are consistent with the initial data in Fig. 3. Since nitrogen is electronically passive toward CuPc and $F_{16}CuPc$, the change in the current under N_2 is ascribed to the desorption of surface dopants. The drain currents of *n*- and *p*-channel devices can be restored completely by storing the devices in dry air over a week. The results suggest that oxygen is a hole donor for MPc *p*-channel ChemFETs and an electron trap agent for *n*-type devices. Therefore, oxygen acts as a dopant in both *p*-type and *n*-type ChemFETs. All analytes we have studied act as hole acceptors in *p*-type ChemFETs and electron donors in *n*-type ChemFETs. Therefore, we describe the behavior of the analytes as "counterdopants" to oxygen consistent with the typical nomenclature used in MOSFET technology.[24]

The role of oxygen doping in the electrical conductivity of MPc materials has been discussed in literature.[25] For CuPc sandwich devices, the electrical conductivity increases by three orders of magnitude after exposure to oxygen.[26] The effect is reversible after prolonged vacuum pumping at elevated temperature or under a H_2 reducing gas flow. The multistep process of oxygen adsorption on MPc surface is proposed in[27]

$$\text{MPc} + \text{O}_2 \overset{K_1}{\leftrightarrow} \text{MPc} - \text{O}_2 \overset{K_2}{\leftrightarrow} \text{MPc}^{\delta+} - \text{O}_2^{\delta-} \overset{K_3}{\leftrightarrow} \text{MPc} - \text{O}_2^- + h^+,$$

$$(1)$$
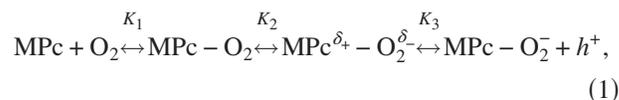
where h^+ are the delocalized hole carriers. The first process is the oxygen adsorption on the MPc surface, the second pro-
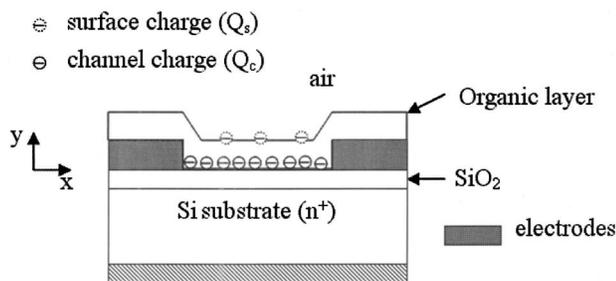
FIG. 4. Device structure of an *n*-channel ChemFET in accumulation mode (not drawn to scale). There are two charge sheets: a thin layer of surface charge (Q_s) at the organic/air interface and channel charge (Q_c) at the organic/SiO$_2$ interface. The surface charge is induced by doping and the sign depends on dopant.

FIG. 5. Chemical responses of *n*-channel F$_{16}$CuPc (a) and *p*-channel CuPc (b) ChemFETs to DMMP in air and N$_2$ at 25 °C. Each DMMP dose is 68 ppm. The bias conditions were *n*-channel ($V_{ds}=+6$ V, $V_{gs}=+8$ V) and *p*-channel ($V_{ds}=-6$ V, $V_{gs}=-8$ V).

cess is the charge transfer between MPc and O$_2$, forming bound superoxide, and the third process is charge delocalization; K_1, K_2, and K_3 are the equilibrium constants for these three processes. For solid-state chemical sensors, the gas adsorption induced current change is related to the change in delocalized carrier density. Therefore, both gas adsorption and charge delocalization steps can be the limiting step in chemical response. Gas physisorption typically has a very low activation energy (≤ 0.3 eV).[28] For the MPc based sensors, steps 2 and 3 were found to be rate limiting in MPc chemiresistors.[29] It is likely that the slow current response due to O$_2$ desorption ($0.7\%/h$) arises from slow charge transfer or delocalization processes [steps 2 and 3 in Eq. (1)].

For organic films over 10 ML thick, gas adsorption primarily occurs at organic/air interface.[26] We found negligible change in the bulk MPc film structure as determine by x-ray diffraction, which is consistent with analytes adsorbing only at the air/organic interface and at grain boundaries, but adsorption at grain boundaries should be a small effect for 10 ML films. Although in thiophene ChemFETs, grain size has been shown to affect sensitivity,[7] we have not observed correlation of chemical sensitivity with grain size in MPc chemical sensors. For the CuPc and F$_{16}$CuPc films grown for this work, the grain size is about 100 nm in diameter. If we assume spherical grains and assume the grains extend through the 10 ML film, the grain boundary surface is estimated to be about 4% of free surface area. Therefore, we have focused on the mechanism of gas adsorption on the surface of MPc films.

We hypothesize that the electronic process of gas adsorption in ChemFETs is a surface doping process. For an *n*-channel ChemFET (see diagram at Fig. 4) in "on" mode, there are two negative charge sheets present in the organic film located at the organic/SiO$_2$ interface (Q_c) and the organic/air interface (Q_s). The negative surface charge is the result of the electrons trapped by oxygen. For a thick ChemFET (>10 ML), the gas surface doping layer and charge transport layer of the transistor are distinct. The chemisorption of analytes primarily occurs on the free surface of the organic film. However, at high gate voltage (~ 10 V above threshold voltage), the charge carrier density of OTFTs accumulates primarily in the first two molecular layers ($>95\%$) above the oxide.[30] Therefore, the electrical
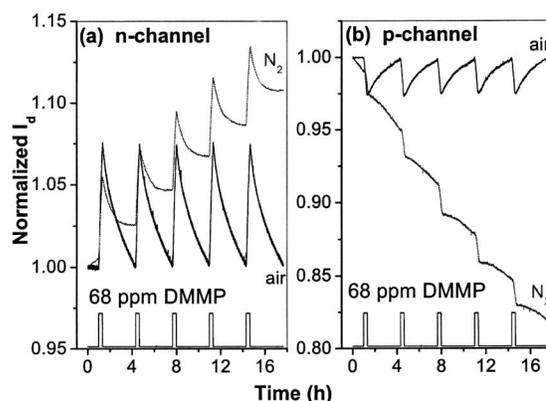
effect of analyte binding to the ChemFET surface is a complicated function of chemisorption and charge transport. The role of oxygen surface doping will be described in Sec. III B.

B. The role of oxygen surface doping on chemical response

Since oxygen has a significant effect on the channel conductivity of MPc ChemFETs, the role of presorbed oxygen on the chemical response was examined. We varied the surface oxygen concentration and compared the chemical responses of two analytes in dry air and N$_2$. The samples were stored in N$_2$ until the baseline current increased 25% for the *n*-channel ChemFET and decreased 25% for the *p*-channel ChemFET. DMMP and MeOH were studied as model analytes. The chemical responses to DMMP (a tight binding analyte) for the two ChemFETs are compared in air and N$_2$ carrier gas (see Fig. 5). MeOH was studied as a model weak binding analyte. The chemical responses to MeOH for the two ChemFETs are also compared in air and N$_2$ carrier gas (see Fig. 6). The time-dependent current plots were normalized to the current at $t=0$ s. We purposely did not allow the devices to completely stabilize after switching from air to N$_2$ ambient because we wanted to measure the influence of oxy-
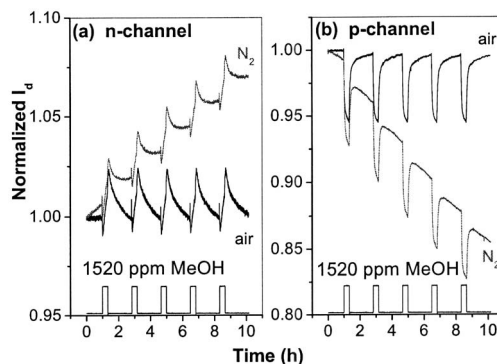
FIG. 6. Chemical responses of *n*-channel F$_{16}$CuPc (a) and *p*-channel CuPc (b) ChemFETs to MeOH in air and N$_2$ at 25 °C. Each MeOH dose is 1520 ppm. The bias conditions were *n*-channel ($V_{ds}=+6$ V, $V_{gs}=+8$ V) and *p*-channel ($V_{ds}=-6$ V, $V_{gs}=-8$ V).
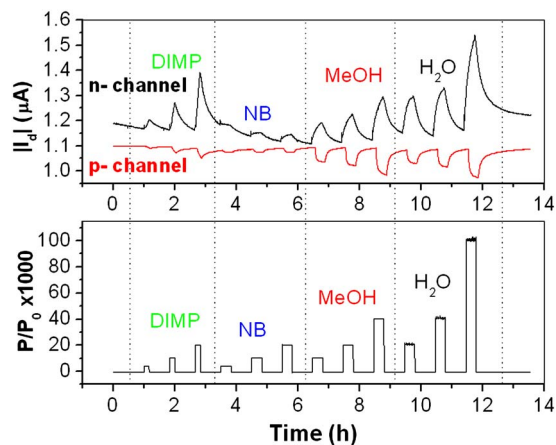
FIG. 7. (Color online) Typical chemical responses of the *n*- and *p*-channel ChemFETs to DIMP, NB, MeOH, and H_2O. The absolute value of *p*-channel ChemFET current was plotted to be in the same scale with the *n*-channel ChemFET. P and P_0 are the partial and saturated pressures of the analytes. The saturated vapor pressures of the analytes at 25 °C are DIMP (93 Pa), MeOH (16 945 Pa), H_2O (3160 Pa), and NB (32 Pa).

gen desorption on the device performance. Furthermore, after complete desorption of oxygen, the *p*-type ChemFETs would have zero current. In these experiments, the baseline drift is employed only to understand the sensing mechanisms since for practical sensing, flat baseline operation is required.

The baseline is recoverable for analyte dosing in N_2 as well as in air and the response to the analytes is approximately opposite for *n*-type and *p*-type films. Any chemical responses due to analyte induced O_2 desorption in N_2 carrier would not be reversible; therefore, since the sloping baseline in N_2 carrier gas is fully recovered after analyte dosing, the results rule out the possibility of DMMP or MeOH causing a change in output current by irreversibly displacing surface bound O_2. Instead, DMMP and MeOH must be acting primarily as counterdopants to O_2. Possible counterdoping mechanisms would include the "coadsorption" or "remote adsorption." (a) Coadsorption: Analytes could be coabsorbing on the same MPc molecule as the O_2 and acting as an electron donor to O_2 so O_2 no longer withdraws charge from the film. (b) Remote adsorption: Analytes could be coabsorb-
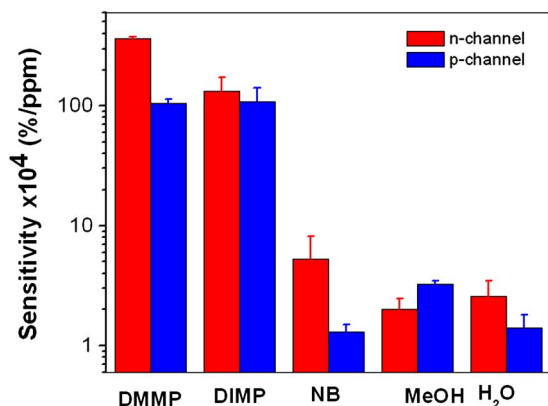
FIG. 8. (Color online) The sensitivities of *n*- and *p*-channel ChemFETs to nerve agent simulants (DMMP and DIMP) and other analytes: MeOH, H_2O, and NB at 25 °C. The sensitivity is in logarithmic scale. Error bars represent standard errors.

ing on a remote site and acting as electronic dopants. In both cases, the analyte may change the surface carrier concentration and/or perturb trap energy of the carrier. We note that in the standard model of organic semiconductors there is no distinction between changing the carrier concentration and perturbing the trap energies.[30]

The responses for the *n*- and *p*-channel ChemFETs in air have been measured with other analytes such as DIMP, nitrobenzene (NB), and H_2O. The chemical responses were measured in the saturated regime at 25 °C and are shown in Fig. 7 for comparison. More detailed study of responses to DMMP and MeOH pulses as a function of concentration will be presented later. For all analytes tested, the responses were of opposite sign between *n*-type and *p*-type ChemFETs. This is consistent with the proposed mechanism by which the analytes change the output current primarily through counterdoping of the surface preadsorbed oxygen. The baseline drift shown in Fig. 7 is attributed to analyte induced drift and has been shown to be minimized using longer recovery times.[17] We have not attempted to optimize the baseline drift shown in Fig. 7; only fixed recovery times were employed for this figure. However, the baselines in Figs. 9 and 10 have been optimized with gate voltage pulse duration and recovery time between chemical pulses. We again note that the recovery time is independent of the presence of ambient oxygen because, as shown in Figs. 5 and 6, the signal recovers even in the complete absence of ambient oxygen.

The chemical responses to five analytes were tested over 8 months. The average chemical sensitivity and standard error values were extracted from six runs and are shown in Fig. 8. The analyte doses (P/P_0) were between 0.005 and 0.1, where P and P_0 are the partial and saturated pressures of the analytes, respectively. Each analyte dose was 20 min long followed by recovery times of 45–180 min. The "approximate" chemical sensitivity was calculated by dividing the percentage current change over the concentration. These are approximate chemical sensitivities since they were calculated over a small concentration range for each analyte. We found that the differences in sensitivities between the analytes exceed the differences in sensitivity between *n*-type and *p*-type ChemFETs. There are differences up to a factor of 3.5 between the approximate sensitivity on the *n*-type and *p*-type ChemFETs, which is consistent with the analytes primarily acting as counterdopants to surface oxygen.

C. Time resolved chemical response and recovery to weak and strong binding analytes

The time resolved chemical responses of *n*- and *p*-channel ChemFETs to DMMP and MeOH in air were compared in more detail. The chemical responses in the form of $\Delta I/I$ are shown in Fig. 9 for side-by-side comparison. The DMMP doses in the experiment were 68 ppm and 20 min long, followed by a 180 min recovery period. The MeOH doses in the experiment were 1520 ppm and 20 min long, followed by a 90 min recovery period. The long recovery times were chosen to ensure identical and fully reversible analyte responses.

It was found that DMMP increases the current of the

TABLE I. The chemical response (R) and desorption constants of n- and p-channel ChemFETs extracted from Fig. 9. The doses were 68 and 1520 ppm for DMMP and MeOH pulses. The pre-exponential and desorption time constants were fitted according to Eqs. (2) and (3). R is in unit of %, τ_1 and τ_2 are in unit of minutes, and A_1 and A_2 have been multiplied by 10^3. The standard deviations for each quantity are shown in the parentheses.

Device	DMMP			MeOH				
	R (%)	τ_1 (min)	A_1	R (%)	τ_1 (min)	A_1	τ_2 (min)	A_2
n	7.64	106.0	117.3	2.41	37.1	37.8	0.89	−11.6
	(0.068)	(3.88)	(2.30)	(0.022)	(0.58)	(0.12)	(0.04)	(0.04)
p	−2.23	100.9	32.4	−5.49	39.1	13.4	3.3	42.6
	(0.075)	(10.35)	(1.68)	(0.026)	(10.86)	(0.36)	(0.14)	(0.67)

n-type F_{16}CuPc device but decreases the current of the p-channel CuPc ChemFET. The percentage current change is referenced to the current at $t=0$ s. At the same dose, the n-channel ChemFET has larger response to DMMP as compared to the p-channel ChemFET. MeOH analyte pulses also induce opposite chemical responses in n- and p-channel ChemFETs. At the same MeOH dose, the p-channel ChemFET has larger response as compared to the n-channel ChemFET, which is opposite to the relative trend for DMMP on p-channel and n-channel devices. There was about 1% current overshoot at the beginning and end of each MeOH pulse in the n-channel ChemFET (see the inset of Fig. 9). The time scales of the overshoots were 130 and 190 s for downward and upward shifts. Therefore, they are unlikely to be caused by the opening and closing of solenoid valves during the vapor delivery. We infer that there two processes occur during MeOH adsorption/desorption on MPc films. The current continued to change even after the analyte was turned off for nearly all analytes. The response delay within 20 s is attributed to the large dead volume of the chamber while larger delays are attributed to the slow desorption of the analyte from the MPc film.

The desorption processes of DMMP and MeOH on CuPc and F_{16}CuPc ChemFETs can be fitted with exponential decay functions. For the DMMP responses, the time evolution of current during analyte desorption was fitted with a first order exponential decay as

$$I_d(t) = I_0 - A_1 \exp\left(\frac{-t}{\tau_1}\right), \qquad (2)$$

where I_0 is the baseline current, A_1 is the pre-exponential coefficient, and τ_1 is the desorption time constant. For MeOH responses on the p-channel ChemFET, the desorption process has to be fitted with a double-exponential process,

$$I_d(t) = I_0 - A_1 \exp\left(\frac{-t}{\tau_1}\right) - A_2 \exp\left(\frac{-t}{\tau_2}\right), \qquad (3)$$

where A_2 and τ_2 are the pre-exponential coefficient and desorption time constant for the second (fast) exponential decay process. We have fitted the desorption of MeOH from n-channel ChemFET with a double exponential with opposite signs for the two pre-exponential coefficients.

The chemical responses and desorption time constants for DMMP and MeOH on CuPc and F_{16}CuPc ChemFETs are tabulated in Table I. The desorption time of MeOH was

shortest among the five analytes we tested. Assuming simple first order kinetics without transport limits, the desorption time is an exponential function of analyte binding energy to MPc molecules. We selected MeOH as a weak binding analyte and DMMP as a strong binding analyte, which has three times longer desorption time. The chemical response (R) was calculated as of the percentage current change to chemical pulses using the current just before each pulse as the reference current. We note that the current continued to change even after the analyte was turned off for some analytes, i.e., the MeOH response of n-channel ChemFETs. Peak values were extracted from Fig. 9. These chemical responses were calculated at a single concentration of analyte, and show that the relative responses of n-channel and p-channel ChemFETs are reversed for DMMP and MeOH.

The desorption time constants for DMMP are nearly identical on n- and p-channel ChemFETs, consistent with DMMP having similar binding strength to CuPc and F_{16}CuPc. We infer that DMMP binds to similar sites in both n- and p-channel films. Therefore, the 3.4 times difference in the DMMP chemical response between n-channel and p-channel is consistent with the differences in the perturbation of the electronic structure of the n- and p-channel MPc films by DMMP.

There is coexistence of fast and slow processes during the adsorption and desorption of MeOH to MPc molecules. The fast component during the adsorption is observed as a
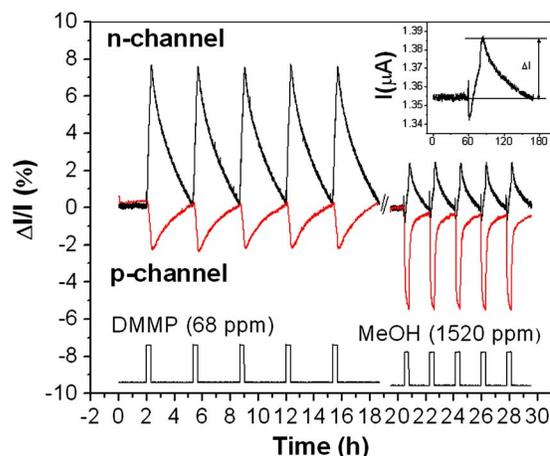
FIG. 9. (Color online) The percentage current change in response to DMMP and MeOH pulses. The DMMP and MeOH analyte pulses are not drawn to scale. The inset shows the time-dependent current plot of response to a methanol pulse.

current overshoot in the *n*-channel ChemFET and as a fast decay in the *p*-channel ChemFET. The slow component acts as an electron donor (or hole acceptor) on both the *n*- and *p*-channel devices, causing a decrease in the magnitude of the current on *p*-channel devices and an increase in magnitude of the current on *n*-channel devices. Conversely, the fast component acts as an electron acceptor on *n*-channel devices and a hole acceptor on *p*-channel devices thereby decreasing the magnitude of the current on both *n*-channel and *p*-channel devices. The time constants for recovery show that the slow component is nearly identical on *n*-channel and *p*-channel devices and the fast component is similar on *n*-channel and *p*-channel devices. The opposite changes in current for *n*-type and *p*-type ChemFETs for slow MeOH response (electron donor) is identical to the other four analytes that were tested. However, the unidirectional changes in current on *n*-type and *p*-type ChemFETs for the fast MeOH response are unusual. One possible type of chemisorption which would be consistent with the unidirectional fast response is charge trapping by MeOH. MeOH is a polar molecule; therefore, it can stabilize holes in *p*-channel devices and electrons in *n*-channel devices when weakly physisorbed to the MPc aromatic rings on the surface. Trapping of free charges in both *n*- and *p*-channel devices should cause a decrease in output current for both types of devices, which is consistent with the observed behavior of the fast process.

Note that there is about a 20-fold difference in the DMMP versus MeOH doses so although the chemical response for DMMP and MeOH appear to be similar in Fig. 9, the actual chemical sensitivity is one order of magnitude
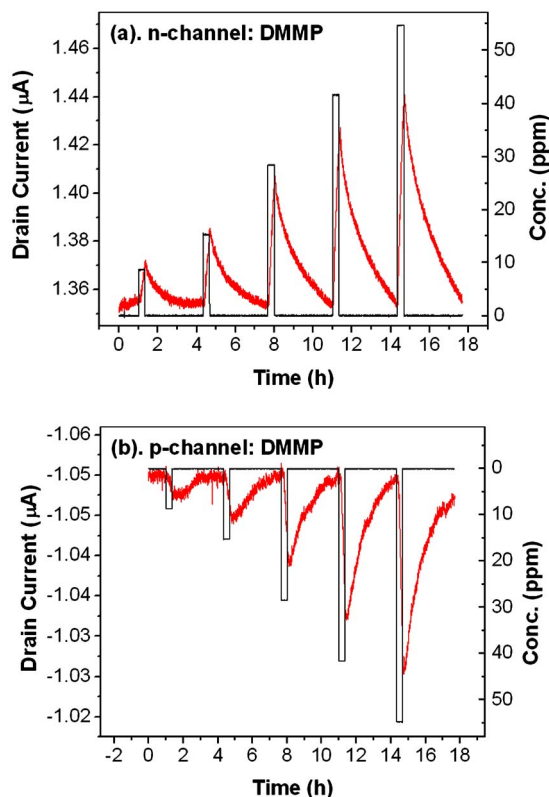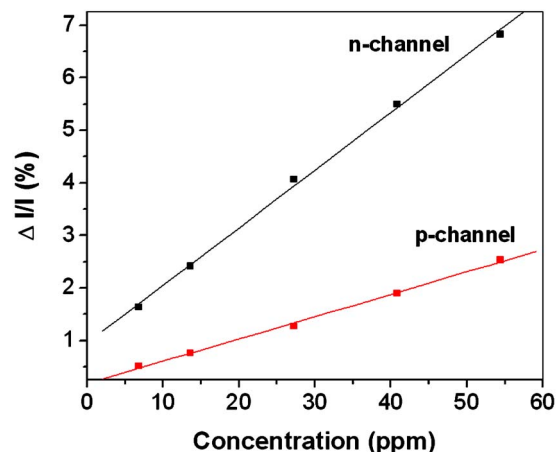
FIG. 11. (Color online) Current changes ($\Delta I/I$) as a function of DMMP concentration at 25 °C in dry air for *n*- and *p*-channel ChemFETs.

higher for DMMP. The greater sensitivity to DMMP compared to MeOH is consistent with stronger binding of DMMP to MPc as suggested by the slower desorption time for DMMP compared to MeOH. The three times difference in desorption time for DMMP versus MeOH on *n*-channel ChemFETs corresponds to a log(3) difference in binding energy and three times difference in surface concentration at identical partial pressure assuming there are no transport limits. Although the diffusion property difference between MeOH and DMMP could partially contribute to the desorption time difference, we have investigated large molecule chemical response times and do not find correlation with molecular weight.[11] Therefore, some of the ten times difference in sensitivity between DMMP and MeOH is due to DMMP more strongly perturbing the electronic structure of the MPc/air interface at an equivalent surface concentration to MeOH.

D. Chemical responses as a function of concentration between *n*- and *p*-channel ChemFETs

The relative sensitivity of the *n*- and *p*-channel ChemFETs to DMMP and MeOH were further investigated as a function of concentration. The chemical responses were measured as a function of DMMP concentration in dry air (see Fig. 10). Each dose was 20 min long followed by 180 min recovery in dry air. All DMMP doses caused a current increase in *n*-channel ChemFETs and a current decrease in *p*-channel ChemFETs. The desorption time constants fitted according to Eq. (2) are 71 ± 22 and 83 ± 21 min for *n*- and *p*-channel ChemFETs, where the errors reflect the variation in desorption times with concentration. Within the error margin of the time constants, the DMMP desorption time constants between *n*- and *p*-channel ChemFETs are comparable.

The chemical response as a function of concentration is extracted from Fig. 10 and shown in Fig. 11. The $\Delta I/I$ has a linear dependence on the DMMP concentration in both devices. It is confirmed that both the *p*-type and *n*-type ChemFETs operate in the kinetically controlled region[11] and have excellent linear dependences on the analyte concentrations. The linear fits of $\Delta I/I$ as a function of DMMP concentration have nonzero interceptions at zero concentration (0.18% and

FIG. 10. (Color online) Chemical responses of *n*-channel F$_{16}$CuPc (a) and *p*-channel CuPc (b) as a function of DMMP concentration at 25 °C.
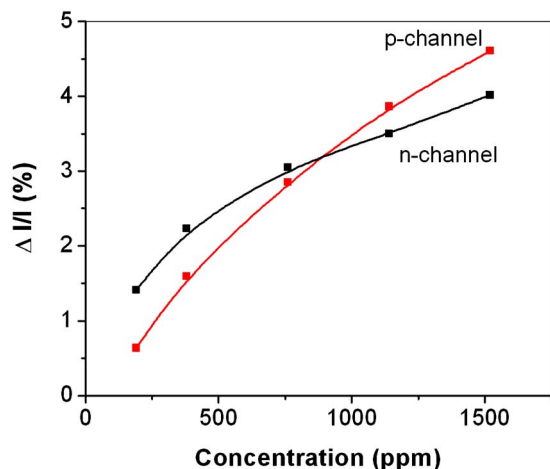
FIG. 12. (Color online) Current changes ($\Delta I/I$) as a function of MeOH concentration at 25 °C in dry air for *n*- and *p*-channel ChemFETs.

0.95% for *p*- and *n*-channel ChemFETs). The nonzero intercepts are due to the nonlinear chemical response at very low DMMP concentration, which might be due to strong analyte binding to defect sites.

Inferred from the above measurements, there is a clear difference between the chemical sensitivity of $F_{16}CuPc$ and CuPc to DMMP. The slope of $\Delta I/I$ versus concentration is 2.5 times larger for the *n*-channel ChemFET. The greater sensitivity to DMMP on *n*-type $F_{16}CuPc$ ChemFETs can be attributed to either stronger binding to the surface of $F_{16}CuPc$ compared to CuPc or to a greater change in electronic structure induced by DMMP on $F_{16}CuPc$ in comparison to CuPc. Since the desorption time constants of DMMP to CuPc and $F_{16}CuPc$ are similar, we ascribed the chemical sensitivity difference solely to the differences in DMMP perturbation of the electron trap energies versus hole trap energies in the *n*-channel and *p*-channel devices.

Similarly, the concentration dependent chemical responses to MeOH are shown in Fig. 12. $\Delta I/I$ values were extracted using the same procedure shown in the inset of Fig. 9. We found that there is nonlinear dependence of chemical response on the MeOH concentration. The nonlinear response is consistent with there being at least two distinct chemisorption mechanisms (slow and fast) for MeOH on the *n*- and *p*-channel devices.

IV. CONCLUSIONS

n-type and *p*-type ChemFETs have been fabricated with $F_{16}CuPc$ and CuPc materials, respectively. The output current drift in air and N_2 is consistent with oxygen acting primarily as surface dopant (electron acceptor) for the *n*- and *p*-channel ChemFETs. Removing oxygen by evacuation or exposure to a stream of nitrogen gas increases the *n*- channel current while decreasing the *p*-channel current. Responses for *n*-channel and *p*-channel ChemFETs were compared for five analytes in air; for all five analytes, the responses were of opposite sign on *n*-type and *p*-type ChemFETs. This is consistent with the primary mechanism being analyte counterdoping of the surface oxygen. The chemical responses to DMMP and methanol at several concentrations in air and N_2

for *n*-type and *p*-type ChemFETs were compared. There is a difference in the chemical sensitivity of 2.5 for DMMP on *p*-type CuPc and *n*-type $F_{16}CuPc$ even though DMMP has a similar binding strength to both MPc films as indicated by the desorption times. The difference in sensitivities between *n*-type and *p*-type films to DMMP is attributed to DMMP exerting a different perturbation of the electron trap energies versus hole trap energies in the *n*-channel and *p*-channel ChemFETs.

[1] L. Torsi and A. Dodabalapur, Anal. Chem. **77**, 380A (2005).
[2] L. Torsi, A. Dodabalapur, L. Sabbatini, and P. G. Zambonin, Sens. Actuators B **67**, 312 (2000).
[3] M. Bouvet, Anal. Bioanal. Chem. **384**, 366 (2006).
[4] R. D. Yang, T. Gredig, J. Park, C. Colesniuc, I. K. Schuller, W. C. Trogler, and A. C. Kummel, Appl. Phys. Lett. **90**, 263506 (2007).
[5] M. Bouvet, G. Guillaud, A. Leroy, A. Maillard, S. Spirkovitch, and F. G. Tournilhac, Sens. Actuators B **73**, 63 (2001).
[6] M. Bora, D. Schut, and M. A. Baldo, Anal. Chem. **79**, 3298 (2007).
[7] T. Someya, H. E. Katz, A. Gelperin, A. J. Lovinger, and A. Dodabalapur, Appl. Phys. Lett. **81**, 3079 (2002).
[8] L. Wang, D. Fine, and A. Dodabalapur, Appl. Phys. Lett. **85**, 6386 (2004); L. Torsi, A. J. Lovinger, B. Crone, T. Someya, A. Dodabalapur, H. E. Katz, and A. Gelperin, J. Phys. Chem. B **106**, 12563 (2002).
[9] A. R. Hopkins and N. S. Lewis, Anal. Chem. **73**, 884 (2001).
[10] E. S. Kolesar, Jr. and J. M. Wiseman, Anal. Chem. **61**, 2355 (1989).
[11] F. I. Bohrer, A. Sharoni, C. Colesniuc, J. Park, I. K. Schuller, A. C. Kummel, and W. C. Trogler, J. Am. Chem. Soc. **129**, 5640 (2007).
[12] J. W. Grate, M. Klusty, W. R. Barger, and A. W. Snow, Anal. Chem. **62**, 1927 (1990).
[13] A. W. Snow and W. R. Barger, *Phthalocyanines Properties and Applications* (Wiley, New York, 1989).
[14] E. Barrena, personal communication (November 2006).
[15] D. G. de Oteyza, E. Barrena, J. O. Osso, S. Sellner, and H. Dosch, J. Am. Chem. Soc. **128**, 15052 (2006); J. Phys. Chem. B **110**, 16618 (2006).
[16] D. G. de Oteyza, E. Barrena, J. O. Osso, H. Dosch, S. Meyer, and J. Pflaum, Appl. Phys. Lett. **87**, 183504 (2005).
[17] Z. A. Bao, A. J. Lovinger, and J. Brown, J. Am. Chem. Soc. **120**, 207 (1998).
[18] M. M. Ling and Z. N. Bao, Org. Electron. **7**, 568 (2006).
[19] R. D. Yang, J. Park, C. N. Colesniuc, I. K. Schuller, W. C. Trogler, and A. C. Kummel, J. Appl. Phys. **102**, 034515 (2007).
[20] M. Knupfer and H. Peisert, Phys. Status Solidi A **201**, 1055 (2004); H. Peisert, M. Knupfer, T. Schwieger, G. G. Fuentes, D. Olligs, J. Fink, and T. Schmidt, J. Appl. Phys. **93**, 9683 (2003).
[21] Z. Bao, A. J. Lovinger, and A. Dodabalapur, Appl. Phys. Lett. **69**, 3066 (1996).
[22] J. Park, R. D. Yang, C. N. Colesniuc, A. Sharoni, S. Jin, I. K. Schuller, W. C. Trogler, and A. C. Kummel, Appl. Phys. Lett. **92**, 193311 (2008).
[23] H. L. Gomes, P. Stallinga, F. Dinelli, M. Murgia, F. Biscarini, D. M. de Leeuw, T. Muck, J. Geurts, L. W. Molenkamp, and V. Wagner, Appl. Phys. Lett. **84**, 3184 (2004).
[24] K. Suzuki, A. Satoh, and T. Sugii, IEEE Electron Device Lett. **17**, 1 (1996).
[25] K. Seki, T. Nishi, S. Tanaka, T. Ikame, H. Ishii, and K. Kanai, Mater. Res. Soc. Symp. Proc. **871E**, I8.11.1 (2005); R. D. Gould, Coord. Chem. Rev. **156**, 237 (1996).
[26] J. D. Wright, Prog. Surf. Sci. **31**, 1 (1989).
[27] M. Passard, C. Maleysson, A. Pauly, S. Dogo, J. P. Germain, and J. P. Blanc, Sens. Actuators B **19**, 489 (1994).
[28] K. W. Kolasinski, *Surface Science* (Wiley, West Sussex, England, 2002).
[29] R. Tongpool and S. Yoriya, Thin Solid Films **477**, 148 (2005).
[30] G. Horowitz, J. Mater. Res. **19**, 1946 (2004).